Journal of
Synchrotron Radiation

ISSN 0909-0495

Received 11 July 2007
Accepted 28 November 2007

Local structure investigation of the active site of the imidazolonepropionase from *Bacillus subtilis* by XANES spectroscopy and *ab initio* calculations

Feifei Yang, Wangsheng Chu, Meijuan Yu, Yu Wang, Sixuan Ma, Yuhui Dong and Ziyu Wu*

Institute of High Energy Physics, Chinese Academy of Sciences, Beijing 100049, People's Republic of China. E-mail: wuzy@ihep.ac.cn

Imidazolonepropionase is an important enzyme that plays a crucial role in the degradation of the histidine in mammals and bacteria. In this contribution a detailed structural investigation is presented of the imidazolonepropionase from *Bacillus subtilis* at the zinc site by X-ray absorption near-edge structure (XANES) spectroscopy combining experimental data with *ab initio* calculation in the framework of the multiple-scattering theory. The resolved local structure leads to a modification of the data set in the Protein Data Bank (PDB) (PDB code 2BB0). Actually, data suggest that the carboxyl of the Asp324 moves far away from the zinc ion at the center, while the water molecule and the nearest-neighbor histidines move towards it. This new conformation and the occurrence of a short water-to-zinc bond length support the nucleophilic attack catalytic mechanism proposed for this enzyme.

© 2008 International Union of Crystallography
Printed in Singapore – all rights reserved

Keywords: imidazolonepropionase; catalysis; XANES; zinc.

1. Introduction

The degradation pathway of histidine in mammals and bacteria follows four steps, each one associated with a specific enzyme: (i) histidine is deaminated to urocanic acid (or urocanate) by histidase; (ii) urocanase converts urocanic acid to 4(5)-imidazone-5(4)-propionic acid (IPA) by the addition of a water molecule; (iii) imidazolonepropionase splits IPA into L-formiminoglutamic acid with another additional water molecule; (iv) the L-formiminoglutamic acid is then turned into free L-glutamic acid by formiminoglutamate hydrolase, involving a third water molecule (Brown & Kies, 1959; Snyder *et al.*, 1961; Kaminskas *et al.*, 1970; Smith *et al.*, 1971). Imidazolonepropionase, on which we focus our attention, is the third enzyme of the above described pathway. Although previous studies revealed that imidazolonepropionase from rat liver has a narrow pH range with maximal activity at pH 7.4 and a Michaelis constant of 7 μM (Snyder *et al.*, 1961), the catalytic mechanism of this enzyme is still not resolved. Recently a three-dimensional structure analysis of imidazolonepropionase from *Bacillus subtilis* with a resolution of about 2.0 Å has been achieved combining X-ray diffraction and protein crystallography (Yu, Li *et al.*, 2006; Yu, Liang *et al.*, 2006). Based on this structure a nucleophilic catalytic mechanism was proposed. In this model the substrate molecule is first bound to the active site through the hydrophilic tunnel of the open conformation of the enzyme, replacing the water that is surrounded by Arg89, Ser329, Glu252, His185 residues and the zinc-bound water. The Zn-bound water is ionized to hydroxide that later launches a nucleophilic attack on the carbonyl carbon of the substrate. Finally, the N—C bond of the substrate breaks and L-formiminoglutamic acid is formed after the amide nitrogen modulates its hybridization (Yu, Liang *et al.*, 2006).

In hydrolase it is fundamental that the coordinated water deprotonates to hydroxide. According to the available Protein Data Bank (PDB) data, the distance between the Zn ion and the catalytic water molecule is 2.38 Å. This distance is associated with the pK_a value of the metal ion, and a shorter Zn—H_2O bond corresponds to a lower pK_a value of the Zn^{2+} ion. Therefore the occurrence of a short Zn—H_2O bond makes easier the ionization of the Zn-bound water. Assuming that for a crystal structure with 2 Å resolution the bond length error is about 0.2–0.3 Å (Ahmed *et al.*, 2007), the determination of the Zn—O(H_2O) bond length of this enzyme is not accurate enough to support the nucleophilic attack catalytic mechanism and a better resolution is mandatory. A software package named *MINUIT XANes* (*MXAN*) has been recently made available. It is capable of determining from the XANES spectrum the local structure of a metalloprotein with high spatial resolution, *i.e.* with a bond length error of about 0.02 Å (Della Longa *et al.*, 2001, 2003; Hayakawa *et al.*, 2004; Benfatto & Della Longa, 2001; D'Angelo *et al.*, 2002; Benfatto *et al.*, 2002; Benfatto & Wu, 2003; Cardelli *et al.*, 2003). Here we

present an XANES analysis at the Zn *K*-edge performed using *MXAN* to determine the local structure around the Zn ion, attempting to complement the existing data sets and to understand the specific catalytic mechanism of the imidazolonepropionase from *Bacillus subtilis*.

2. XAS spectra

X-ray absorption spectroscopy (XAS) is a sensitive local probe of atomic structure. As a consequence it is really a unique and accurate method of investigating the active site structure in metalloproteinases, such as copper proteins (Hasnain & Hodgson, 1999; Hasnain & Strange, 2003; Wang *et al.*, 1998; Banci *et al.*, 2005), ferric or ferrous proteins (Della Longa *et al.*, 2001, 2003; Benfatto *et al.*, 2003; Conradson *et al.*, 1994; Stone *et al.*, 2005; Nordlander *et al.*, 1993; Shu *et al.*, 1997; Hwang *et al.*, 2000), zinc proteins (Hasnain & Hodgson, 1999; Feiters *et al.*, 2003), lead proteins (Magyar *et al.*, 2005), manganese proteins (Webb *et al.*, 2005) *etc*. Actually XANES spectroscopy is an effective method of determining the local structure around a metal ion at high resolution, and experiments can be performed on samples in any physical state (Della Longa *et al.*, 2001; Hwang *et al.*, 2000; Feiters *et al.*, 2003; Magyar *et al.*, 2005; Webb *et al.*, 2005; Pasquarello *et al.*, 2001). For the analysis of the XANES data we applied the *MXAN* package which has been developed to extract both metrical and angular structural information from an experimental spectrum of complex systems, such as metalloproteins (Della Longa *et al.*, 2001, 2003; Hayakawa *et al.*, 2004; Benfatto & Della Longa, 2001; D'Angelo *et al.*, 2002; Benfatto *et al.*, 2002; Benfatto & Wu, 2003; Cardelli *et al.*, 2003).

3. Experiments

A solution of imidazolonepropionase from *Bacillus subtilis* with a pH value around the maximal activity (pH 7.5) was provided by the team of Xiao-Dong Su of Peking University (Yu, Liang *et al.*, 2006). X-ray absorption spectra at the Zn *K*-edge were collected in the fluorescence yield mode at the X-ray absorption station of the 4W1B beamline of the Beijing Synchrotron Radiation Facility. The storage ring was working at 2.2 GeV and experiments were performed at room temperature with an electron current decreasing from 120 to 80 mA during a time span of about 8 h. The incident beam intensity was monitored using an ionization chamber flowed by a gas mixture composed of 25% argon and 75% nitrogen, while the fluorescence signal was collected by means of a Lytle detector filled with argon gas. The solution was kept in a cell sealed by Kapton films and with a Teflon spacer of 1.2 mm. To monitor the radiation damage of the monochromatic radiation at the Zn *K*-edge, we performed tests on fresh samples. Data collected on a time scale of 2 min did not show any detectable differences from the consecutive XAS scans, suggesting that the dose release in these XAS experiments is too low to modify the local structure of the enzyme.

4. *MXAN* calculations

To extract detailed structural information around the Zn ion site, we applied *MXAN*, a code capable of performing a quantitative analysis of an XANES spectrum, *i.e.* from the absorption edge up to 200 eV, *via* comparison of the experimental data with theoretical calculations obtained by changing relevant geometrical parameters of the atomic site (D'Angelo *et al.*, 2002; Webb *et al.*, 2005; Pasquarello *et al.*, 2001). *MXAN* searches the minimum of the square residue function in the space of the parameters defined as

$$S^2 = n \frac{\sum_{i=1}^{m} w_i \left[\left(y_i^{\rm th} - y_i^{\rm exp} \right) \varepsilon_i^{-1} \right]^2}{\sum_{i=1}^{m} w_i},$$

where n is the number of independent parameters, m is the number of data points, $y_i^{\rm th}$ and $y_i^{\rm exp}$ are the theoretical and experimental absorption values, respectively, ε_i is the individual error in the experimental data set and w_i is a statistical weight. Actually, when w_i = a constant = 1, the square residual function S^2 reduces to the statistical χ^2 function. The X-ray absorption cross sections have been calculated using the full multiple-scattering scheme in the framework of the muffin-tin approximation for the shape of the potential (Natoli & Benfatto, 1986; Wu *et al.*, 1996). In particular, the exchange and correlation part of the potential have been determined on the basis of the local density approximation of the self energy. Inelastic processes have been taken into account by a convolution with a Lorentzian function having an energy-dependent width of the form $\Gamma(E) = \Gamma_{\rm c} + \Gamma_{\rm mfp}(E)$. In this way the constant part $\Gamma_{\rm c}$ accounts for both the core–hole lifetime (1.8 eV) (Fuggle & Inglesfield, 1992) and the experimental resolution (1.5 eV), while the energy-dependent term represents the intrinsic and extrinsic inelastic processes (D'Angelo *et al.*, 2002; Benfatto & Wu, 2003; Roscioni *et al.*, 2005). The muffin-tin radii were chosen according to the Norman criterion with a 15% overlap (Norman, 1974; Joly, 2001). This method takes into account multiple-scattering events in a rigorous way through the evaluation of the scattering path operator (Natoli & Benfatto, 1986; Wu *et al.*, 2001), and its reliability has been successfully tested in different systems (D'Angelo *et al.*, 2002; Benfatto *et al.*, 2002; Benfatto & Wu, 2003).

In Fig. 1(*a*) we compare the Zn *K*-edge XANES spectrum of the imidazolonepropionase from *Bacillus subtilis* with a *MXAN* calculation of a 51-atom cluster based on the crystallographic conformation (model A). The simulation with S^2 = 30.6, shown in Fig. 1(*a*), is in poor agreement with the experimental data, indicating the occurrence of significant differences with the real structure. In Fig. 1(*b*) we show the best fit (continuous black line) again obtained using *MXAN* with the geometrical parameters of the relevant atoms set free to move. This second simulation is characterized by S^2 = 1.78 and the nearest atomic structure (model B) has been outlined in Fig. 2 using thick yellow sticks. This second structure shows that the catalytic water molecule and three nearest-neighbor

histidines move towards the center ion while the carboxyl of the Asp324 moves away from it. The bond angle differences between the nearest ligands and the bond lengths of the two models are summarized in Tables 1 and 2, respectively.

We fit two other structures using the same 51-atom cluster as model A. However, in these additional sets the water distances were longer, *i.e.* 2.15 Å and 2.25 Å, while all other atoms were allowed to move freely. Their S^2 values are 2.14 and 3.12, respectively. Therefore we may recognize that although the spectrum with the Zn—O(water) distance fixed at 2.15 Å is better, it is not as good as the spectrum related to the fit without restriction in Fig. 1(*b*). In other words, a structure with a shorter Zn–water distance better resembles the local conformation at the Zn site of the enzyme.

Table 1
Comparison of the bond angles among the five closest ligands to the Zn^{2+} ion.

Data of model B from this work and model A relative to the PDB data set are summarized above and below the diagonal, respectively.

	N(His82)	N(His80)	N(His249)	O(COO)	O(H_2O)
N(His82)		107.3 ± 3.5	105.0 ± 2.5	83.1 ± 2.5	114.4 ± 2.5
N(His80)	109.6		96.3 ± 3.5	80.8 ± 3.5	127.5 ± 3.5
N(His249)	100.0	90.6		171.9 ± 2.5	102.0 ± 1.0
O(COO)	91.4	80.5	167.4		74.3 ± 2.5
O(H_2O)	119.8	125.2	102.3	76.1	

Table 2
Comparison of the main bond distances (in Å) of the available structures of the imidazolonepropionase from *Bacillus subtilis*.

	Zn—His82	Zn—His80	Zn—His249	Zn—Asp324	Zn—H_2O
From PDB	2.18	2.19	2.28	2.32	2.38
From *MXAN*	2.04 ± 0.02	2.06 ± 0.02	2.20 ± 0.02	2.55 ± 0.02	2.04 ± 0.02

5. Results and discussion

Because the functional aspect of imidazolonepropionase from *Bacillus subtilis* is related to the structure around the metal ion, this investigation attempted to reconstruct the local stereochemistry around the Zn site. Looking at the bond angles, model A summarized in Table 1 is a distorted trigonal bipyramid with the catalytic water, the His80 and His82 residues in the equatorial plane and the axial His249 and Asp324 residues. Since angles between axial His249 and the three ligands in the equatorial plane are 100.0°, 90.6° and 102.3°, the Zn ion is out of the equatorial plane and slightly oriented towards the His249 ligand. The distortion increases in model B where the axial-equatorial angles become 105.0°, 96.3° and 102.0°, respectively. Assuming that model B is a distorted tetrahedron, the angles between the four ligands, *e.g.* the three histidines and the water molecule excluding the Asp324 residue, are all around 109°, *i.e.* 107.3°, 105.3°, 114.4°, 127.5°, 96.3° and 102.3°, respectively. Therefore it is reasonable to consider model B as mainly four-coordinated.

Among the available PDB structures with resolution higher than 1.5 Å we found 11 Zn-contained hydrolases all characterized by a similar local structure in which Zn is bound to a catalytic water molecule and more than two histidines. Seven of these structures are four-coordinated while only one is five-coordinated. Although the above data set is limited, it supports the hypothesis that Zn prefers a four-coordinated geometry such as Zn—N_3O to a five-coordinate Zn—N_3O_2 structure. As listed in Table 2, the four nearest bonds of the zinc ion, *e.g.* Zn—His80, Zn—His82, Zn—His249 and Zn—H_2O, are characterized by bond lengths shorter by 0.14 Å,

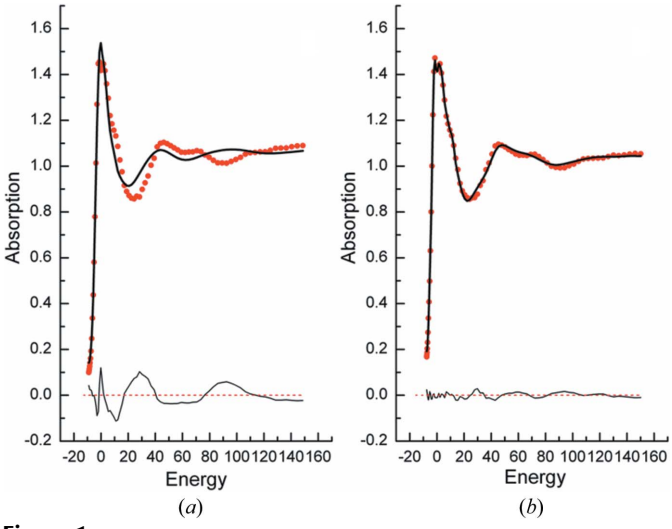

Figure 1
Comparison of the experimental Zn *K*-edge XANES spectrum (dots), the XANES simulation of the structure of the model A (left, continuous line) and the XANES best fit (right, continuous line). The difference between the experimental data and the corresponding calculation (continuous line) is shown at the bottom of each panel.

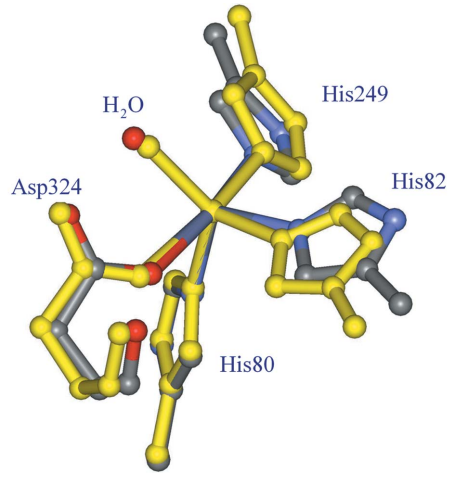

Figure 2
Comparison of two Zn local structural models: model A, which is based on the diffraction data (colored sticks), and model B, which is obtained by the *MXAN* analysis (yellow sticks). Only nearest ligands are shown.

0.13 Å, 0.08 Å and 0.36 Å, respectively, while the Zn—γO (Asp324) bond length is 0.22 Å longer. In structures with similar local conformations the Zn—H_2O bond ranges between 1.93 Å and 2.07 Å, with only three cases exhibiting bond distances longer than 2.10 Å. Moreover, the Zn—O distance in most of the four-coordinate and six-coordinate zinc compounds is around 1.96 Å and 2.08 Å, respectively. Because the Zn—O(water) bond length of this enzyme (2.04 Å) falls between these two limits, it is reasonable to consider that a strong interaction between the catalytic water and the zinc ion occurs similarly to the Zn—O bond in most inorganic zinc compounds.

As shown in Fig. 3, a short length in protein scaffolding generates secondary interactions, inducing His80 and His249 residues to form a hydrogen bond with the γ-carboxyl of the Asp271 and Asp219, respectively. The occurrence of hydrogen bonds can strengthen the complexation of the zinc ion (Christianson & Alexander, 1989; Auld, 1997), playing a relevant role in the stabilization of the zinc site, a mechanism that is also responsible for the reduced Zn—N bond length (the sum of the van der Waals radii of N and Zn is 2.93 Å) and Zn—O(H_2O) bond length. Moreover, a catalytic triple interaction has been previously reported, and refers to the particular interaction between a histidine ligand, zinc and a γ-carboxyl group of the Asp residue (Christianson & Alexander, 1989; Auld, 1997). As a consequence, we may consider that the zinc ion, together with the His80 and Asp271 (or His249 and Asp219) residues, form a catalytic triad in the imidazolonepropionase from *Bacillus subtilis*. In addition, the catalytic water molecule lies among three histidines, the zinc ion and a γ-carboxylate of the Asp324, all of which are Lewis bases. Based on the particular structure, the catalytic water molecule must be active for ionization, which is probably responsible for the strong interaction between catalytic water and the zinc ion. The evolution from the Zn-bound water to Zn—OH is able to increase the nucleophilicity of the zinc. Based on the information described above, we may claim that a short Zn–water bond is more compatible with the occurrence of deprotonation of the catalytic water and better supports the occurrence of the proposed nucleophilic attack catalytic mechanism (Yu, Liang *et al.*, 2006).

6. Conclusions

We have investigated the metalloprotein imidazolonepropionase from *Bacillus subtilis* (PDB code 2BB0) by XANES spectroscopy. Thanks to the high accuracy of the method, an accurate revised structure is presented and discussed in consideration of the catalytic mechanism of the enzyme (Yu, Li *et al.*, 2006; Yu, Liang *et al.*, 2006). From our analysis, the bond length between the Zn ion and the catalytic water molecule is 0.36 Å shorter than that available in the PDB. Moreover, instead of a five-coordinated Zn active site as previously recognized, an XANES fit performed using the *MXAN* package showed that it tends to four-coordinated. Finally, data indicate that the catalytic water is bound to the central Zn ion with a very short bond. As a consequence, the catalytic water can be easily deprotonated and turned into hydroxyl, providing structural support to the model that a Zn–hydroxyl bond acts as a nucleophilic reagent to the carbonyl carbon.

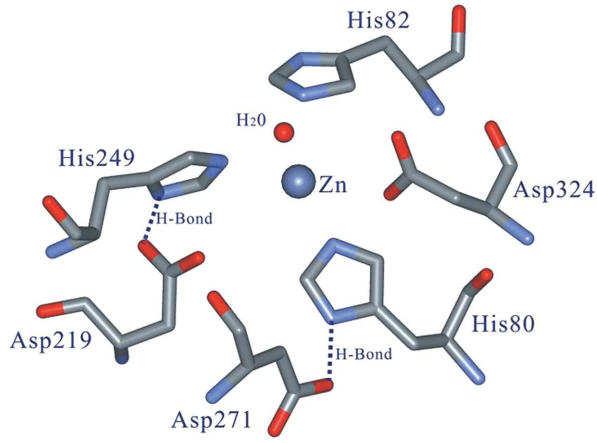

Figure 3
Schematic layout of the characteristic hydrogen bonds occurring between the His and Asp residues.

This work was supported by the National Outstanding Youth Fund (Project No. 10125523 to ZW) and the Key Important Project of the National Natural Science Foundation of China (10490190, 10490191 and 10490193). A sincere acknowledgment is due to Yamei Yu who gently provided us with samples for the experiments and the structural information of the PDB model. A special thanks is due to A. Marcelli and M. Benfatto for many fruitful discussions.

References

Ahmed, H. U., Blakeley, M. P., Cianci, M., Cruickshank, D. W. J., Hubbard, J. A. & Helliwell, J. R. (2007). *Acta Cryst.* D**63**, 906–922.
Auld, D. S. (1997). *Structure and Bonding*, Vol. 89, *Zinc Catalysis in Metalloproteases*. Berlin/Heidelberg: Springer Verlag.
Banci, L., Bertini, I., Ciofi-Bafoni, S., Katsari, E., Katsaros, N., Kubicek, K. & Mangani, S. (2005). *Proc. Natl. Acad. Sci.* **102**, 3994–3999.
Benfatto, M., D'Angelo, P., Della Longa, S. & Pavel, N. V. (2002). *Phys. Rev. B*, **65**, 174205.
Benfatto, M. & Della Longa, S. (2001). *J. Synchrotron Rad.* **8**, 1087–1094.
Benfatto, M., Della Longa, S. & Natoli, C. R. (2003). *J. Synchrotron Rad.* **10**, 51–57.
Benfatto, M. & Wu, Z. Y. (2003). *Nucl. Sci. Tech.* **1**, 11–21.
Brown, D. D. & Kies, M. W. (1959). *J. Biol. Chem.* **234**, 3188–3191.
Cardelli, A., Cibin, G., Benfatto, M., Della Longa, S., Brigatti, M. F. & Marcelli, A. (2003). *Phys. Chem. Miner.* **30**, 54–58.
Christianson, D. W. & Alexander, R. S. (1989). *J. Am. Chem. Soc.* **111**, 6412–6419.
Conradson, S. D., Burgess, B. K., Newton, W. E., Di Cicco, A., Filipponi, A., Wu, Z. Y., Natoli, C. R., Hedman, B. & Hodgson, K. O. (1994). *Proc. Natl. Acad. Sci.* **91**, 1290–1293.
D'Angelo, P., Benfatto, M., Della Longa, S. & Pavel, N. V. (2002). *Phys. Rev. B*, **66**, 064209.
Della Longa, S., Arcovito, A., Benfatto, M., Congiu-Castellano, A., Girasole, M., Hazemann, J. L. & Lo Bosco, A. (2003). *Biophys. J.* **85**, 549–558.

Della Longa, S., Arcovito, A., Girasole, M., Hazemann, J. L. & Benfatto, M. (2001). *Phys. Rev. Lett.* **87**, 155501.
Feiters, M. C., Eijkelenboom, A. P. A. M., Nolting, H.-F., Krebs, B., van den Ent, F. M. I., Plasterk, R. H. A., Kaptein, R. & Boelens, R. (2003). *J. Synchrotron Rad.* **10**, 86–95.
Fuggle, J. C. & Inglesfield, J. E. (1992). *Unoccupied Electronic States, Topics in Applied Physics*, Appendix B, p. 347. Berlin: Springer.
Hasnain, S. S. & Hodgson, K. O. (1999). *J. Synchrotron Rad.* **6**, 852–864.
Hasnain, S. S. & Strange, R. W. (2003). *J. Synchrotron Rad.* **10**, 9–15.
Hayakawa, K., Hatada, K., D'Angelo, P., Della Longa, S., Natoli, C. R. & Benfatto, M. (2004). *J. Am. Chem. Soc.* **126**, 15618–15623.
Hwang, J., Krebs, C., Huynh, B. H., Edmondson, D. E., Theil, E. & Penner-Hahn, J. E. (2000). *Science*, **287**, 122–125.
Joly, Y. (2001). *Phys. Rev. B*, **63**, 125120.
Kaminskas, E., Kimhi, Y. & Magasanik, B. (1970). *J. Biol. Chem.* **245**, 3536–3544.
Magyar, J. S., Weng, T.-C., Stern, C. M., Dye, D. F., Rous, B. W., Payne, J. C., Bridgewater, B. M., Mijovilovich, A., Parkin, G., Zaleski, J. M., Penner-Hahn, J. E. & Godwin, H. A. (2005). *J. Am. Chem. Soc.* **127**, 9495–9505.
Natoli, C. R. & Benfatto, M. (1986). *J. Phys. (Paris) Colloq.* **47**(C8), 11–23.
Nordlander, E., Lee, S. C., Cen, W., Wu, Z. Y., Natoli, C. R., Di Cicco, A., Filipponi, A., Hedman, B., Hodgson, K. O. & Holm, R. H. (1993). *J. Am. Chem. Soc.* **115**, 5549–5558.
Norman, J. G. (1974). *Mol. Phys.* **81**, 1191–1198.
Pasquarello, A., Petri, I., Salmon, P., Parisel, O., Car, R., Toth, E., Powell, D. H., Fischer, H. E., Helm, L. & Merbach, A. E. (2001). *Science*, **291**, 856–859.
Roscioni, O. M., D'Angelo, P., Chillemi, G., Della Longa, S. & Benfatto, M. (2005). *J. Synchrotron Rad.* **12**, 75–79.
Shu, L., Nesheim, J. C., Kauffmann, K., Munck, E., Lipscomb, J. D. & Que, L. (1997). *Science*, **275**, 515–518.
Smith, G. R., Halpern, Y. S. & Magasanik, B. (1971). *J. Biol. Chem.* **246**, 3320–3329.
Snyder, S. H., Silva, O. L. & Kies, M. W. (1961). *J. Biol. Chem.* **236**, 2996–2998.
Stone, K. L., Behan, R. K. & Green, M. T. (2005). *Proc. Natl. Acad. Sci.* **102**, 16563–16565.
Wang, Y., Dubois, J. L., Hedman, B., Hodgson, K. O. & Stack, T. D. P. (1998). *Science*, **279**, 537–540.
Webb, S. M., Dick, G. J., Bargar, J. R. & Tebo, B. M. (2005). *Proc. Natl. Acad. Sci.* **102**, 5558–5563.
Wu, Z. Y., Ouvrard, G., Lemaux, S., Moreau, P., Gressier, P., Lemoigno, F. & Rouxel, J. (1996). *Phys. Rev. Lett.* **77**, 2101–2104.
Wu, Z. Y., Xian, D. C., Natoli, C. R., Marcelli, A. Mottana, A. & Paris, E. (2001). *Appl. Phys. Lett.* **79**, 1918–1920.
Yu, Y., Liang, Y.-H., Brostromer, E., Quan, J.-M., Panjikar, S., Dong, Y.-H. & Su, X.-D. (2006). *J. Biol. Chem.* **281**, 36929–36936.
Yu, Y., Li, L., Zheng, X., Liang, Y.-H. & Su, X.-D. (2006). *Biochim. Biophys. Acta*, **1764**, 153–156.